The Mean Surface Water Balance over Africa and Its Interannual Variability

S. E. NICHOLSON, J. KIM, AND M. B. BA

Department of Meteorology, The Florida State University, Tallahassee, Florida

A. R. LARE

Applied Research Corporation, NASA/GSFC, Greenbelt, Maryland

(Manuscript received 18 March 1996, in final form 24 December 1996)

ABSTRACT

This article presents calculations of surface water balance for the African continent using a revised version of the Lettau climatonomy. Calculations are based on approximately 1400 rainfall stations, with records generally covering 60 yr or longer. Continental maps of evapotranspiration, runoff, and soil moisture are derived for January, July, and the annual mean. The model is also used to provide a gross estimate of the interannual variability of these parameters over most of the continent and local water balance calculations for a variety of locations in Africa. The results are compared with four other comprehensive global water balance studies. The results of this study are being used to produce a 1 × 1 gridded dataset for the continent, with potential applications for numerical modeling studies.

1. Introduction

The important role of the hydrologic cycle in global weather and climate has become increasingly recognized, as the creation of the international Global Energy and Water Cycle Experiment program attests (Chahine 1992a,b). Numerous studies have demonstrated that accurate representation of surface hydrology can improve weather forecasts (e.g., Walsh et al. 1985). Hydrologic feedbacks modify the interannual variability over land (Entekhabi et al. 1992) and dramatically influence ocean–atmosphere interactions (Webster 1994). Recycled water can contribute as much as 50% of the atmospheric water vapor over continents (Brubaker et al. 1993). Such feedbacks may have played a role in intensifying and prolonging the drought in the West African Sahel (Nicholson 1989).

During the past decade, considerable effort has been put into the representation of hydrologic processes in numerical models. The recent project for the Intercomparison of Land Surface Parameterization Schemes has uncovered significant shortcomings, particularly in runoff calculations (Pitman et al. 1993). In one comparison, model predictions of runoff for the "wet" month of August ranged from 30 to over 400 mm. Model improvements require accurate surface hydrologic data for initialization, boundary conditions, and validation.

Unfortunately, parameters such as evapotranspiration (ET) or runoff are rarely measured directly. The few measurements that exist are at local or basin scale. Evapotranspiration is generally calculated from empirical formulas or energy balance approaches. Runoff is generally calculated as a residual. Few data are available for continental- or global-scale comparisons.

The best-known comprehensive studies of global water balance are those of Baumgartner and Reichel (1975), Willmott et al. (1985), Henning (1989), and Mintz and Walker (1993). Henning's calculations are based on empirical formulas derived by Albrecht (1951, 1962) from data for one station in the Gobi Desert; maps of ET, runoff, and various radiative parameters are drawn manually from station records. Baumgartner and Reichel (1975) produce maps of evapotranspiration and runoff from the station data produced by Thornthwaite and associates (e.g., Mather 1962–65). Both studies use station data that are irregularly distributed and cover in many cases only a few years. Willmott et al. (1985) basically use the Thornthwaite method for calculations, but improve on the dataset; they present ET and soil moisture, but not runoff. Mintz and Walker (1993) use a simple water balance model with precipitation and potential evapotranspiration as input. Both of these last two studies extrapolate the areal integrals best suited for the gridded weather and climate models, but produce maps with only very coarse resolution (4 lat × 5 long).

In this paper, we present calculations of surface water balance for the African continent, using a new, more

Corresponding author address: Dr. Sharon E. Nicholson, Dept. of Meteorology, B-161, The Florida State University, Tallahassee, FL 32306-3034.
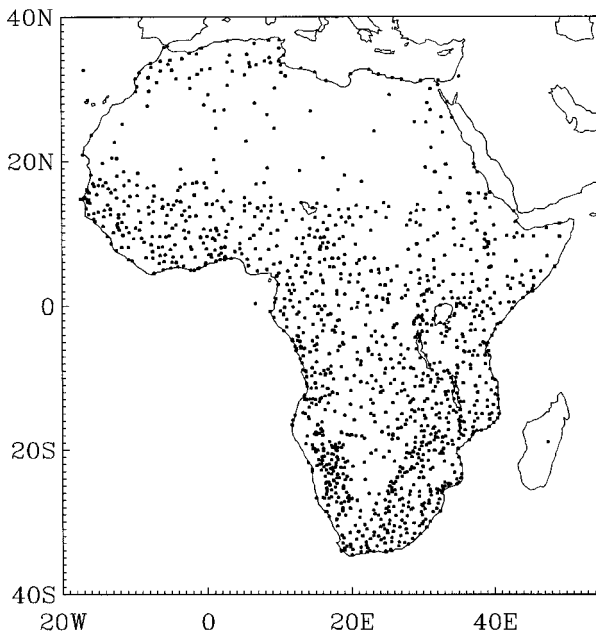
FIG. 1. Distribution of rainfall stations used to calculate water balance.

physically based approach than previous studies and a more comprehensive dataset. Continental maps of evapotranspiration, runoff, and soil moisture are derived using the "evapoclimatonomy" model of surface water balance (Nicholson et al. 1996a). Calculations also provide a gross estimate of the interannual variability of these parameters over most of the continent and local water balance calculations for a variety of locations in Africa. Emphasis is placed on the drought-prone West African Sahel, a region where surface hydrology appears to play a major role in modulating the interannual variability of climate. The results of this work are being used to produce a 1 1 gridded dataset that will be available through an anonymous File Transfer Protocol server through the Department of Meteorology at The Florida State University (ftp.met.fsu.edu).

2. Methodology

a. Data

The basic input is precipitation data for nearly 1400 stations that are reasonably well distributed over the African continent (Fig. 1). This archive has been collected, processed, and updated by the first author over many years and used in numerous research applications (e.g., Nicholson 1994). Quality control tests have been performed and resulted in discarding about 5% of the data. Except for desert regions, the network is sufficiently dense that nearly all 1 1 grid squares include one or more stations. Areal estimates and precipitation fields based on these stations are

nearly identical to those derived from high-resolution satellite data (Ba et al. 1995; Nicholson et al. 1996b).

The water balance calculations utilize long-term means of precipitation calculated as the arithmetic mean of data for all available years. The annual mean and means for January and July are shown in Fig. 2. Because of the strong interdecadal variability of rainfall over parts of Africa, most notably the Sahel, we have found the mean thus derived to be more stable than, for example, means for a standard 30-yr period. Three-quarters of the station records commence prior to 1925, and most records have been updated to 1990 or later. Thus, in most cases, the long-term mean refers to a period of 60 yr or longer. The subsequently calculated water balance parameters also represent means for these multidecadal periods.

Other input data required for the climatonomy model are indicated in Fig. 3, showing an overview of the climatonomy model and the climate and radiative parameters and soil and vegetation information needed for its application. The geographic information derives from sources used extensively in current land–atmosphere models, such as the S:B model, Biosphere–Atmosphere Transfer Scheme (BATS), and others. Radiative parameters are calculated from satellite data.

Vegetation information is derived from two sources: 1) Advance Very High Resolution Radiometer data from the National Oceanic and Atmospheric Administration polar-orbiting satellites are used to calculate the Normalized Difference Vegetation Index (NDVI), with a resolution of approximately 7.6 km, and 2) the Dorman and Sellers (1989) vegetation dataset, which includes 12 vegetation types, has a 5 5 resolution, and provides gross estimates of type, coverage, and emissivity. The NDVI data were provided by C. J. Tucker of the Global Inventory, Monitoring, and Modeling Studies group at National Aeronautics and Space Administration Goddard and are described in more detail in Nicholson and Farrar (1994).

Soils information, including texture, organic matter, and cation exchange capacity, is taken from Zobler (1986) and Webb et al (1991). Produced for climate models, the data have a 1 1 resolution.

The radiative parameters, global radiation at the surface, and surface albedo were derived from Meteosat data for each station location. These represent means for the period from 1983 to 1988. The estimation of these data is described in two companion articles by M. Ba et al. (1997, manuscript submitted to *J. Climate*) and M. Ba and S. Nicholson (1997, manuscript submitted to *J. Climate*, hereafter BN97). The resolution of these data is 0.25 0.25 . Potential evapotranspiration was taken from FAO (1984).

The resolution of the input datasets is varied, ranging from several kilometers to 5 of latitude and longitude. However, all datasets but the Dorman and Sellers vegetation dataset have a resolution of at least 1 1 . For those data, coarse resolution is sufficient because the mod-
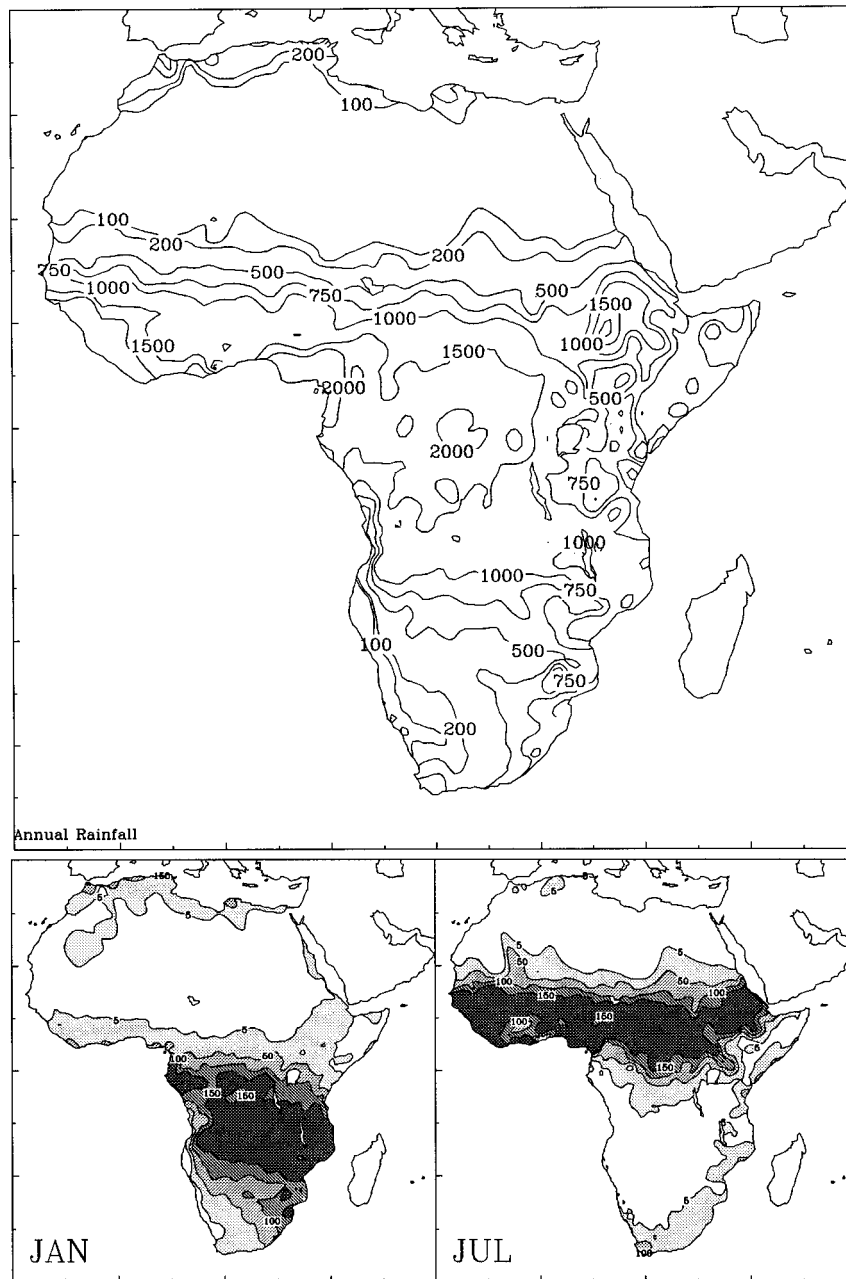
FIG. 2. Mean rainfall (in mm) over Africa from 1950 to 1989. Top: annual mean. Bottom left: January mean. Bottom right: July mean.

el shows little sensitivity to vegetation cover and emissivity, but is considerably more sensitive to NDVI (Marengo et al. 1996). There is also a variation of time periods represented by the input data, with long-term average precipitation being utilized, while satellite data represent an average of about a decade of recent years. However, the interannual variability of radiation parameters is considerably smaller than that of precipitation (BN97) and the model does not show strong sensitivity to NDVI, so that the input data can be considered as long-term means compatible with the precipitation estimates.

b. The evapoclimatonomy model

Monthly and annual values of evapotranspiration, runoff, and soil moisture are calculated by a surface water balance model termed evapoclimatonomy. This is a revised version of the quasi-empirical model originally developed by Lettau (1969) and Lettau and Baradas (1973). Details of the model and model equations have recently been published in a number of sources (e.g., Lare and Nicholson 1994; Nicholson et al. 1996a; Marengo et al. 1996), and hence only a brief overview is
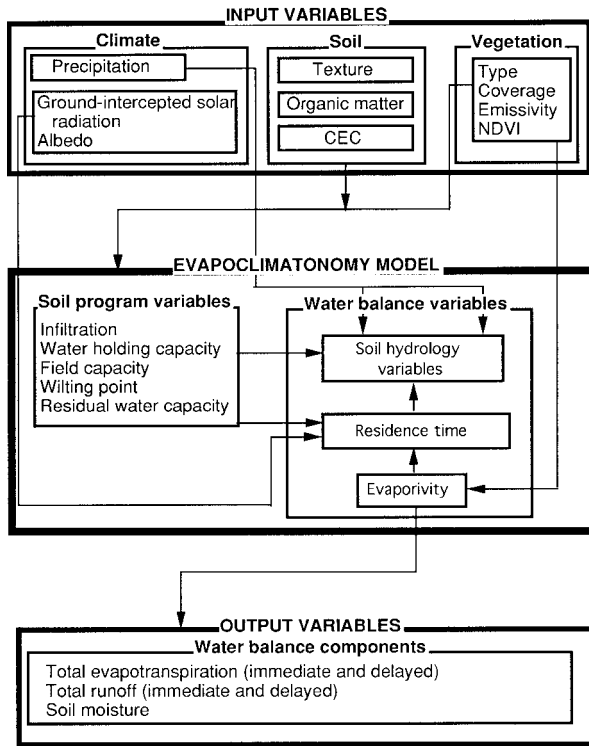
FIG. 3. Overview of the evapoclimatonomy model used to calculate water balance parameters in this study.

presented here. The model was validated using data for the Hydrological Atmospheric Pilot Experiment (HAPEX)-Sahel experiment, conducted over the central Sahel in 1992 (Nicholson et al. 1997; Marengo et al. 1996).

The evapoclimatonomy submodel is essentially a numerical solution to a simplified form of the hydrologic balance equation:

$$P = E + N + \frac{dm}{dt}, \qquad (1)$$

where P is precipitation, E is evapotransipration, N is runoff, and dm/dt is the change in soil moisture storage. Three assumptions are made in order to maintain simplicity (Lare and Nicholson 1990). The first is that for a continental region with a stable climate there is no net storage of moisture over sufficiently long time periods (i.e., for the multiyear period for which means of forcing functions are derived). Therefore,

$$\overline{P} = \overline{E} + \overline{N}. \qquad (2)$$

The second assumption is that the processes of runoff and evapotranspiration can be further subdivided into immediate ( ) and delayed (ь) parts. Thus,

$$E = E + E_{\flat} \qquad (3)$$

and

$$N = N + N_{\flat}. \qquad (4)$$

Immediate processes are those that occur in the same

month as the precipitation, while "delayed" implies processes that are associated with the rain that fell in previous months. For evapotranspiration, E roughly corresponds to the contribution of soil evaporation and the evaporation of intercepted–detained surface moisture, while $E_{\flat}$ is roughly the transpirational component, which draws from the deeper soil moisture reservoirs. For runoff, the partitioning roughly corresponds to surface runoff versus gravitational drainage.

The final assumption of the evapoclimatonomy submodel is that the delayed processes vary directly in proportion to soil moisture according to

$$N_{\flat}(t) = \frac{\overline{N_{\flat}} m(t)}{\overline{m}} \qquad (5)$$

and

$$E_{\flat}(t) = \frac{\overline{E_{\flat}} m(t)}{\overline{m}}, \qquad (6)$$

where $\overline{N_{\flat}}$ and $\overline{E_{\flat}}$ are the mean quantities of delayed runoff and evapotranspiration. These quantities are combined in such a way as to yield a process parameter known as "residence time" t^*:

$$t^* = \frac{\overline{m}}{\overline{N_{\flat}} + \overline{E_{\flat}}}. \qquad (7)$$

This represents the time required for a volume of water equal to the annual mean of exchangeable soil moisture to be depleted by the delayed processes of runoff and evapotranspiration.

With these considerations, the resultant hydrologic balance formula is

$$P = E + N + \frac{m}{t^*} + \frac{dm}{dt}. \qquad (8)$$

By subtracting the annual means from each term in the above equation, an ordinary differential equation results:

$$P'(t) = \frac{m - \overline{m}}{t^*} + \frac{d(m - \overline{m})}{dt}, \qquad (9)$$

where

$$P'(t) = P - E + N - (\overline{P} - \overline{E} - \overline{N}). \qquad (10)$$

This is solved as

$$m = \overline{m} + e^{-t/t^*}\left[\text{constant} + \int e^{t/t^*}p'\,dt\right]. \qquad (11)$$

Because of the initial assumption of climatic stability, the bracketed term must approach 0, thus determining the integration constant.

This model requires the parameterization of immediate and delayed evapotranspiration and runoff and the estimation of two model parameters, the residence time t^* and a second process parameter termed evaporivity e^*, representing the efficiency at which solar radiation

is used in the evaporation process. Immediate runoff N is calculated following Warrilow (1986), using infiltration capacity and rainfall; delayed runoff $N_{\cdot}$ is calculated as gravitational drainage, using the hydraulic conductivity and soil moisture content. Immediate evapotranspiration E is calculated as the product of evaporivity and precipitation, prorated by the ratio of monthly to annual absorbed solar radiation for the month in question; $E_{\cdot}$ is calculated as a residual.

The calculation of the process parameters e^* and t^* is more empirically based. Residence time t^* is calculated after Serafini and Sud (1987) as a function of potential evapotranspiration, wilting point, and field capacity, with an adjustment of values for various vegetation types. Wilting point and field capacity are determined according to Saxton et al. (1986) as a function of soil type (i.e., percentage of sand and clay content). The evaporivity e^* is defined as a nonlinear measure of the capacity of the land surface to use a portion of monthly solar radiation to evaporate precipitation received in the same month. It serves the same function as potential evaporation in traditional water balance models and is analytically derived by using the Normalized Difference Vegetation Index (see Lare 1992).

In earlier versions of the model (Lare and Nicholson 1990, 1994; Nicholson and Lare 1990; Farrar et al. 1994), the soil moisture estimate only refers to exchangeable soil moisture (m)—that is, that available for the processes of runoff and evapotranspiration. The residual water content (rwc) must be added to the calculated exchangeable soil moisture to obtain the true soil moisture contents. Residual water content is determined after Rawls and Brakensiek (1989):

$$\text{rwc} \quad 10[0.2 \quad 0.1(\% \text{ om})$$
$$0.25(\% \text{ clay})(\text{cec})^{0.45}]d, \qquad (12)$$

where rwc is the residual water content in millimeters, (% om) is the percentage of organic matter content, (% clay) is the percentage of clay content, (cec) is cation exchange capacity, and d is the bulk density of the entire soil layer (0–100 cm).

c. Model validation and sensitivity studies

Our version of the climatonomy model was validated at the daily and monthly timescales using data from the HAPEX-Sahel experiment (Marengo et al. 1996; Nicholson et al. 1996c). Sensitivity studies were also carried out by Marengo et al. (1996) and Nicholson and Lare (1990). Results from application to a millet site and a fallow guiera bush site in the central Sahel for the experiment period of August to October 1992 are shown in Table 1. The measured soil moisture values represent an integral of the 1-m layer of soil, which the model-calculated soil moisture is assumed to represent.

Excellent agreement is found for the millet field, with differences depending on whether or not the model was forced with average rainfall for the experimental ''su-

TABLE 1. Comparisons between modeled and observed soil moisture for the SS supersite. Observations are from HAPEX-Sahel and were integrated for the 100-cm layer by using neutron probes at 10-, 20-, 25-, 30-, 40-, 60-, 80-, and 100-cm depth (available for August–October 1992 only). One asterisk indicates that the model was run with rainfall averaged at a supersite scale (seven stations per supersite); two asterisks indicate that the model was run with rainfall for stations inside the local field (three stations inside the local field). Units are millimeters. (From Marengo et al. 1996.)

	Millet, SS			Fallow guiera, SS		
	Model*	Model**	Observations	Model*	Model**	Observations
August	77.6	70.5	81.8	90.6	108.1	111.9
September	83.9	74.6	79.9	94.2	121.8	100.7
October	56.4	54.0	47.5	60.1	70.9	56.2

persite'' or for the local field. In the latter case, the difference between modeled and measured rainfall is about 4 mm in the months of August and September, when measured soil moisture is about 80 mm. Differences are slightly larger for October for model runs forced with more localized rainfall.

The model results for the fallow field with guiera compare somewhat less favorably with measurements. Measured soil moisture is 112 and 101 mm, respectively, for August and September; the model calculations for August are 91 and 108 mm for the supersite and local rainfall, respectively, while those for September are 94 and 122 mm, respectively.

3. Results

a. Mean maps

Annual average evapotranspiration and monthly averages for January and July are shown in Fig. 4. The 100-mm contour roughly bounds the Sahara on the north, its location varying from about 31 to 35 N, and on the south it is located at 18 to 20 N. The 500-mm contour is situated near 15 N, running through Lake Chad. The position of both contours is essentially identical to that of the corresponding rainfall isohyets (Fig. 2), indicating low runoff throughout this region. Throughout most of the Tropics, from about 12 N to 12 S, annual evapotranspiration exceeds 1000 mm; in three humid cores closer to the equator, it exceeds 1500 mm, reaching 2000 mm in the wettest areas. Reduced values are evident on the eastern margins of these latitudinal zones, reflecting the more arid climates of eastern Africa, with evapotranspiration on the order of 500 to 750 mm. In the semiarid subtropics of southern Africa, it generally ranges between 200 and 750 mm, with small values reflecting the Namib Desert and the karoo of South Africa.

Monthly values reflect the annual march of the ITCZ and the rainy season over Africa. In July, evapotranspiration exceeds 100 mm in a core region extending roughly between the equator and 15 N. It exceeds 50
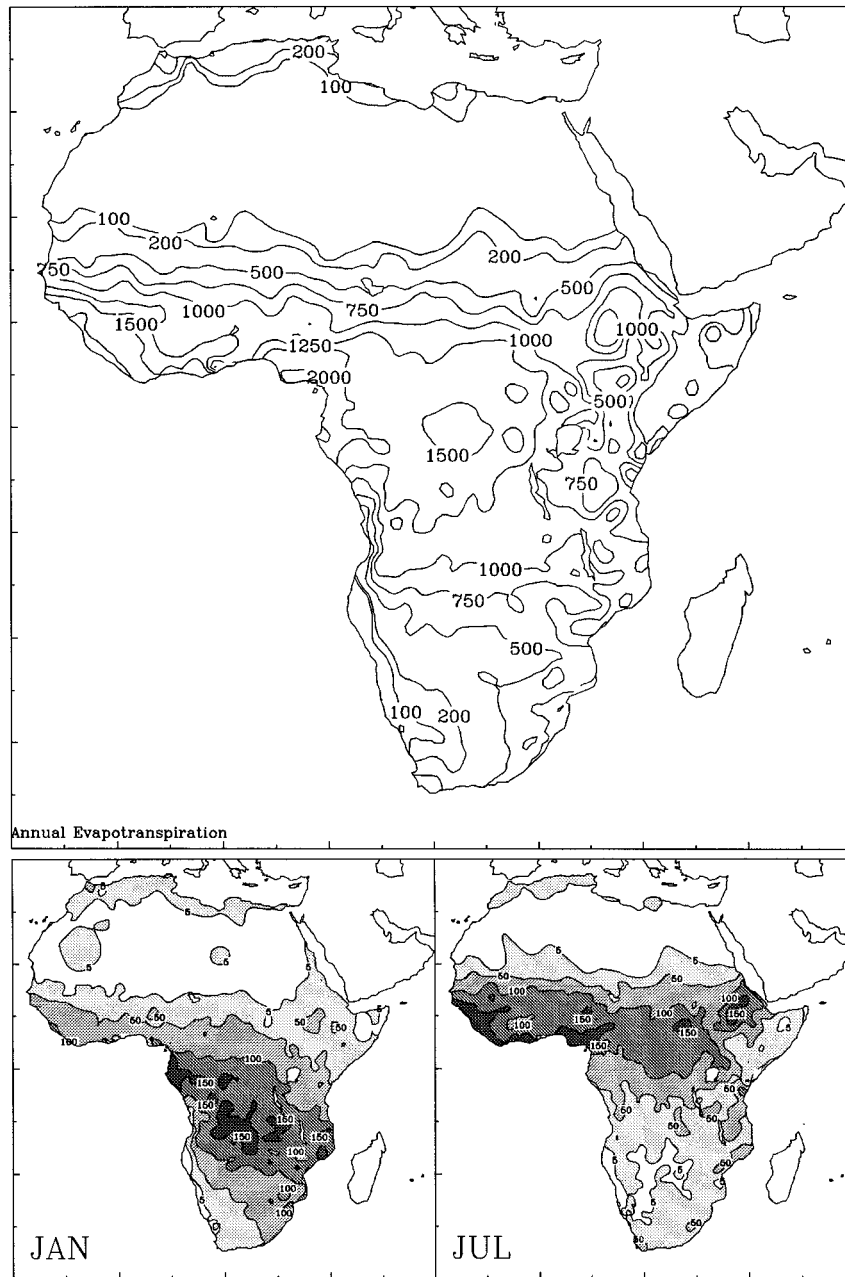
Fig. 4. Mean evapotranspiration over Africa, as calculated by the evapoclimatonomy model. Top: annual mean (mm yr⁻¹). Bottom left: January mean (mm month⁻¹). Bottom right: July mean (mm month⁻¹).

mm from there to about 18 N and 5 S. In the southern Sahel of West Africa (12 to 15 N), it is on the order of 50 to 100 mm, and it is 5 to 50 mm in the northern Sahel (15 to 18 N). Elsewhere, it is generally in the range of 5 to 50 mm, except for the desert areas of the Sahara, the Namib, and the central Kalahari. Within the central Sahara, it exceeds 5 mm in two locations, a western sector where winter rainfall is not uncommon and the Tibesti highlands to the notheast of Lake Chad.

In January, the zone of maximum ET is shifted south-ward, with values exceeding 100 mm roughly from the equator to 20 S. In the southern Sahel, ET has fallen to 5 to 50 mm during January. Values below 5 mm are evident in a much broader area surrounding the Sahara and including the northern Sahel, but are restricted to small coastal desert sectors in the Southern Hemisphere. In both months, it is on the order of 5 to 50 mm in northern Africa.

Runoff is shown in Fig. 5. In the annual mean, the 1-mm contour extends to roughly 15 N, indicating no
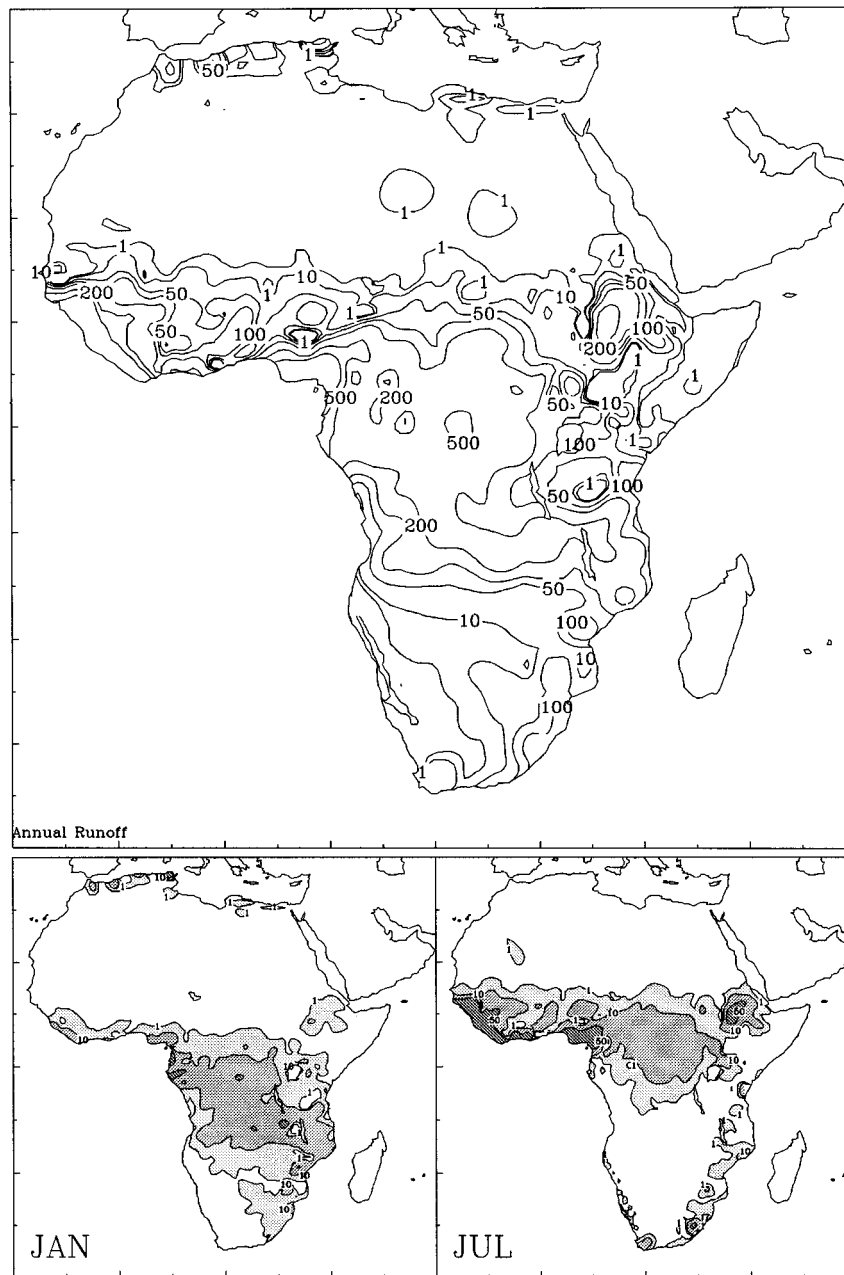
FIG. 5. Mean runoff over Africa, as calculated by the evapoclimatonomy model. Top: annual mean (mm yr $^{-1}$). Bottom left: January mean (mm month $^{-1}$). Bottom right: July mean (mm month $^{-1}$).

surface runoff in the northern Sahel. North of the desert, it lies near 35 N, bounding small moutainous areas in the northwest, where runoff can reach 50 mm. In tropical latitudes, excluding eastern equatorial Africa, runoff is on the order of 200 to 500 mm. In semiarid southern Africa, annual runoff ranges from about 10 to 200 mm, but there is a strong gradient between 10 and 15 S, so that it is below 50 mm throughout most of the region. It approaches zero in the Namib, southern Kalahari, and the karoo.

As with evapotranspiration, monthly values reflect the annual march of the ITCZ and the rain belt. The core region, with values exceeding 10 mm month $^{-1}$, migrates from the northern Tropics in July to the southern Tropics in January. It exceeds 50 mm only during July in areas along the Guinea coast of West Africa.

Soil moisture is shown in Fig. 6. It generally ranges, in the annual mean, from about 10 mm in the Sahelo–Saharan region to over 200 mm in an equatorial core
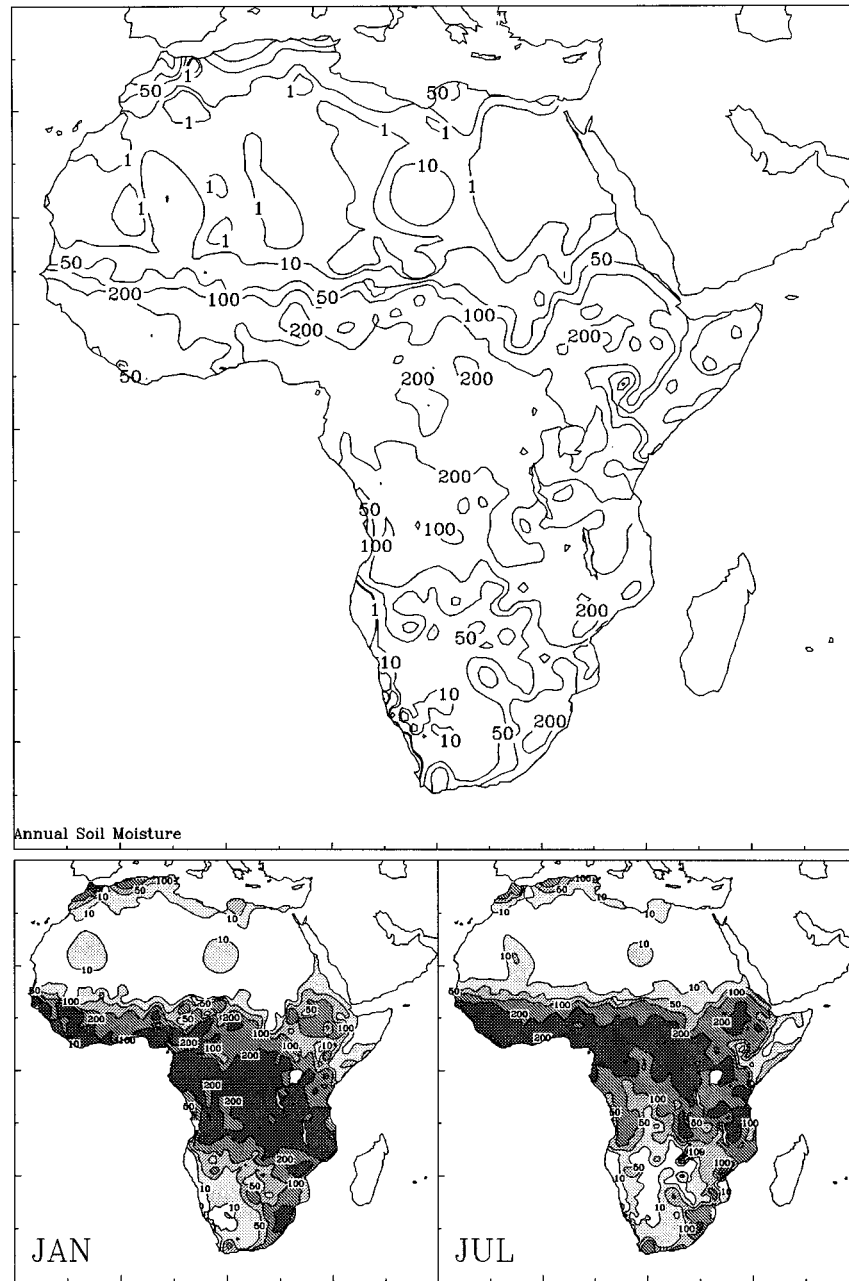
FIG. 6. Mean exchangeable soil moisture (in mm) over Africa, as calculated by the evapo-climatonomy model. Top diagram: annual mean. Bottom left: January mean. Bottom right: July mean.

extending from roughly 10 N to 5 S. It ranges from about 10 to 50 mm in the semiarid Kalahari and the karoo of southern Africa, but falls well below 10 mm in the Sahara and the coastal deserts of southern Africa. These same ranges are evident in January and July, but the areas of maxima and minima are displaced, slightly northward in July and considerably southward in January.

b. Local water balance

The mean water balance for seven diverse locations in Africa is shown in Fig. 7. Algiers, along the Mediterranean coast, receives winter rainfall. The stations Tahoua, Sikasso, Gagnoa, and Bambesa represent a gradual transition from the "summer" rainfall region of the Sahel, through the savanna and woodlands, to the
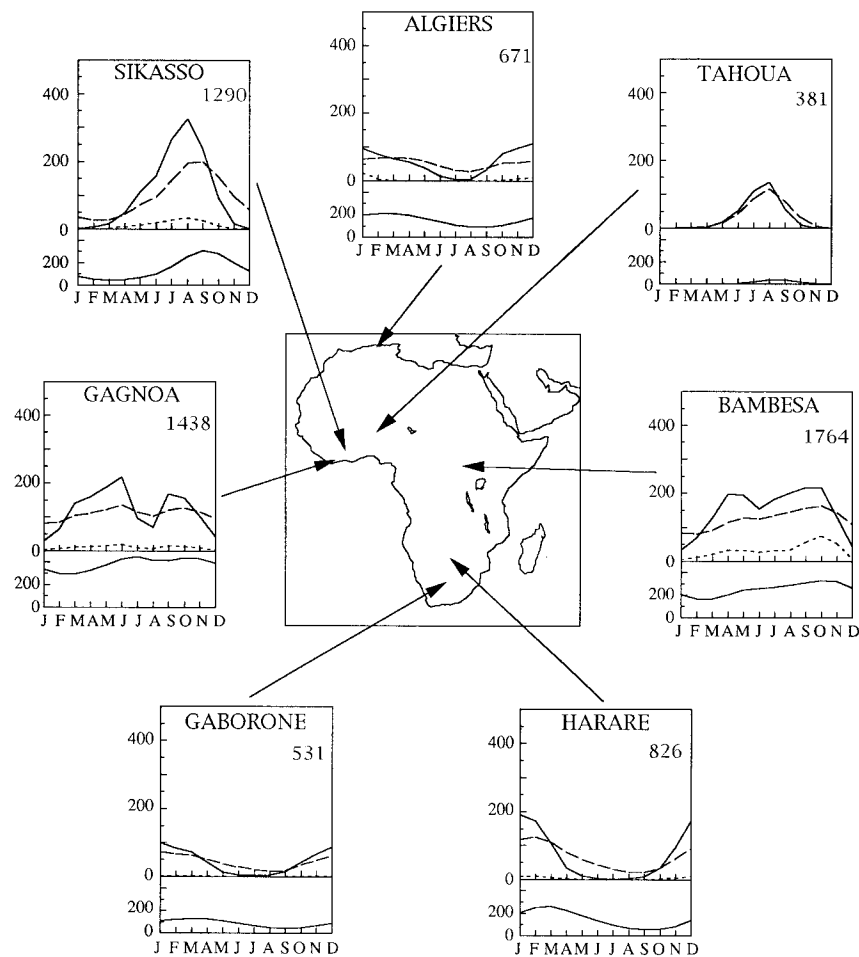
FIG. 7. Mean water balance at seven diverse African locations. Top diagram: solid line is rainfall, dashed line is evapotranspiration, and dotted line is runoff, all in mm month [1]. Bottom diagram: mean monthly exchangeable soil moisture in millimeters. Mean annual rainfall (in mm) is given in the upper right.

equatorial forest with year-round rains. Harare and Gaborone represent the Southern Hemisphere analogs to the Sahel, savanna regions with summer rainfall.

Runoff is almost negligible at Algiers, where the winter rains are frontal in nature and, therefore, low in intensity, promoting infiltration and subsequent evapotranspiration. Consequently, evapotranspiration continues throughout the dry season, drawing on the soil reservoir of moisture. Thus, the magnitude of the annual cycle of ET is considerably lower than that of rainfall. At Tahoua, in the northern Sahel, runoff is essentialy zero; local runoff may occur and collect in internal drainage ponds, from which it later evaporates. Evaporation exceeds rainfall during 3 months, but is negligible much of the year.

In the more tropical latitudes, runoff is considerably greater. At Sikasso, with a single, intense rainy season, it reaches about 30 mm month [1] during August. There, ET exceeds rainfall during about half of the year and reaches a maximum of nearly 200 mm month [1] in Au-

gust and September. At Gagnoa, with roughly the same amount of rainfall, there are two, less intense rainy seasons and consequently lower peak runoff. Since both rainy seasons are preceded by dry seasons, the soil does not become strongly saturated, a contributing factor to the relativley low amounts of runoff. At Bambesa, with year-round rainfall, the soil moisture continues to increase throughout the season, and hence both ET and runoff continue to increase throughout the rainy season. Evapotranspiration reaches about 130 mm month [1] during the first peak in the rainy season, but about 170 mm month [1] during the second, broader peak. Runoff reaches about 30 mm month [1] during the first peak, compared with about 80 mm month [1] during the second.

At the Southern Hemisphere savanna stations, the picture is quite different. The rainy season is longer than in Sahelian locations, with comparable annual amounts, and therefore peak values of rainfall and ET are considerably lower. At Harare, rainfall reaches approximately 170 to 190 mm in 3 months, while ET does not
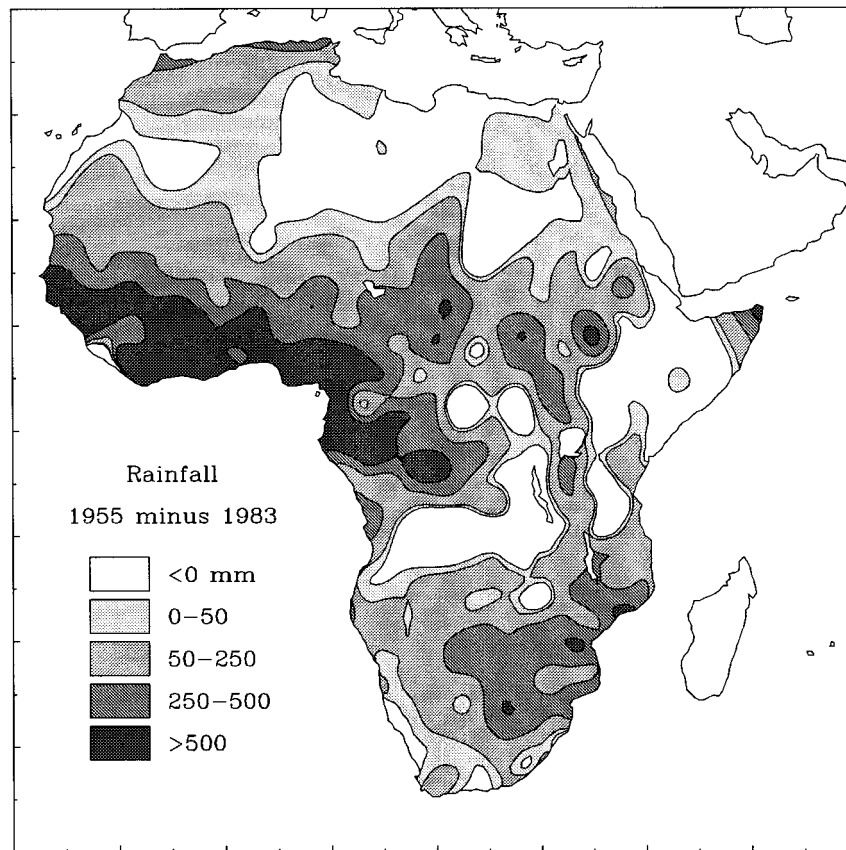
FIG. 8. Difference (in mm) between annual rainfall in 1955 and 1983, continentally an
exceedingly wet and an exceedingly dry year, respectively.

exceed 125 mm. Evapotranspiration continues through-
out the long dry season. At Gaborone, rainfall barely
reaches 100 mm month $^{-1}$ and ET does not exceed 70
mm month $^{-1}$, but, as at Harare, continues throughout
the dry season. This contrast with other tropical loca-
tions is due to the nature of the rain-bearing systems.
In southern Africa, these are often frontal in nature,
reflecting significant midlatitude influences; convective
systems prevail elsewhere. The water balance at Ga-
borone, with a "tropical" summer rainfall regime, is
similar to that at Algiers, with an extratropical winter
rainfall regime. The most apparent difference is higher
dry season evapotranspiration at Algiers, a consequence
of its occurrence during the summer, compared to the
winter dry season at Gaborone.

c. Interannual variability

The African continent is well known for the extreme
interannual variability of rainfall, particularly in the
semiarid subtropics. This produces complex changes in
the surface water balance. These changes might be mod-
ulated by the interannual variability of other parameters,
most notably solar radiation. However, the changes of
rainfall are of a considerably greater magnitude. Thus,

to provide a simple illustration of the rough magnitude
of interannual variability of water balance parameters,
the differences between values for one continentally wet
year and one continentally dry year are shown in Figs.
8, 9, and 10. For select locations, calculations on a
monthly scale are done for the 10 wettest and 10 driest
years and compared to the long-term mean (Figs. 11
and 12).

Over most of the continent, rainfall in 1955 exceeded
that in 1983, with the difference exceeding 250 mm in
large areas. The exceptions are areas of the Sahara,
where differences are negligible, and parts of equatorial
Africa, where 1955 was actually the drier of the two
years. Other than at these locations, these two years
provide a reasonable estimate of the magnitude of in-
terannual variability of evapotranspiration and runoff.

The excess rainfall during 1955 results in nearly the
same excess in ET throughout most of the continent.
Only in equatorial regions are differences distinguish-
able from the relatively coarse map in Fig. 9. Thus, ET
varies by hundreds of millimeters from year to year over
large sectors of Africa.

Large differences in runoff are apparent only in trop-
ical latitudes and in areas of relatively high elevation:
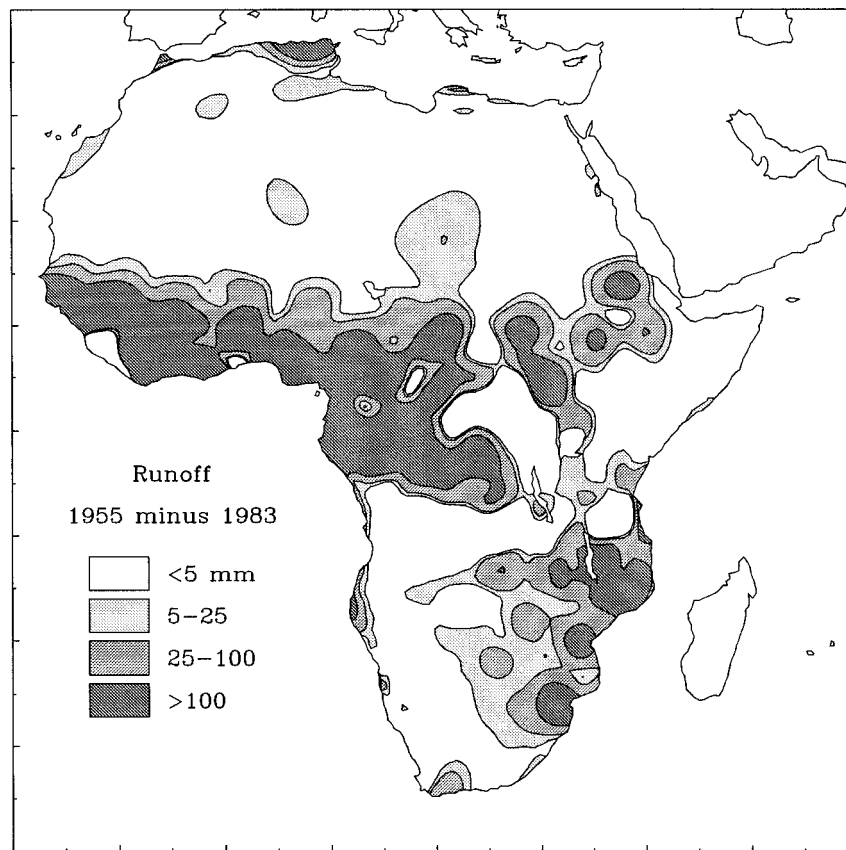the Mediterranean coast, the Ethiopian highlands, coast-

FIG. 9. Difference (in mm) between annual runoff in 1955 and 1983, continentally an exceedingly wet and an exceedingly dry year, respectively.

al sectors of Angola, and the eastern half of the southern subcontinent. In these areas, the interannual variability of runoff is on the order of 25 to over 100 mm. North of approximately 15 N—that is, in the northern Sahel—the difference is negligible, with the increased rainfall in 1955 being totally manifested as increased evapotranspiration. This characteristic was noted earlier by Lare and Nicholson (1994), who pointed out the resultant change in the latitudinal gradient of latent heating across West Africa, an effect potentially large enough to modulate the interannual variability of rainfall.

Figure 11 underscores the interannual variability of runoff via calculations for the wettest and driest years at six of the locations shown in Fig. 7. An asymmetry is clearly apparent, with runoff not changing markedly during the dry years, but being dramatically enhanced during the wet years. At the low-latitude stations of Gagnoa and Bambesa, this difference can be 150 to nearly 300 mm month⁻¹. At Harare in southern Africa, similar differences are apparent in March. Differences are small in the more arid locations.

For evapotranspiration, the monthly differences at these stations (Fig. 12) are more symmetric between dry and wet years. During the wettest months, the difference

between dry and wet years is on the order of 100–150 mm. An interesting trend is observed at Gagnoa, where ET has two peaks during the year in the mean and during the driest year, but esssentialy one peak from August to October during the wettest year. The latter probably reflects a diminished dry season intensity during the wet year and a continual increase in soil moisture throughout the season. A similar pattern is observed in the mean at Bambesa, the wettest station. However, during the wettest year at Bambesa, the two-peaked pattern in ET emerges, probably a manifestation of higher rainfall earlier in the year, when the sun is nearly overhead and radiation (and hence potential ET) is high.

d. Long-term trends

The long-term trends in rainfall and runoff are shown in Fig. 13 for each 10 of latitude from 40 S to 40 N for the period 1950–89. These depict broad continental-scale trends, but may not capture some more local patterns in cases where climate anomalies are not zonally oriented, such as the subtropics of southern Africa. Annual rainfall and runoff are calculated for the calendar year (January to December) by averaging the annual values at all stations in the zone.
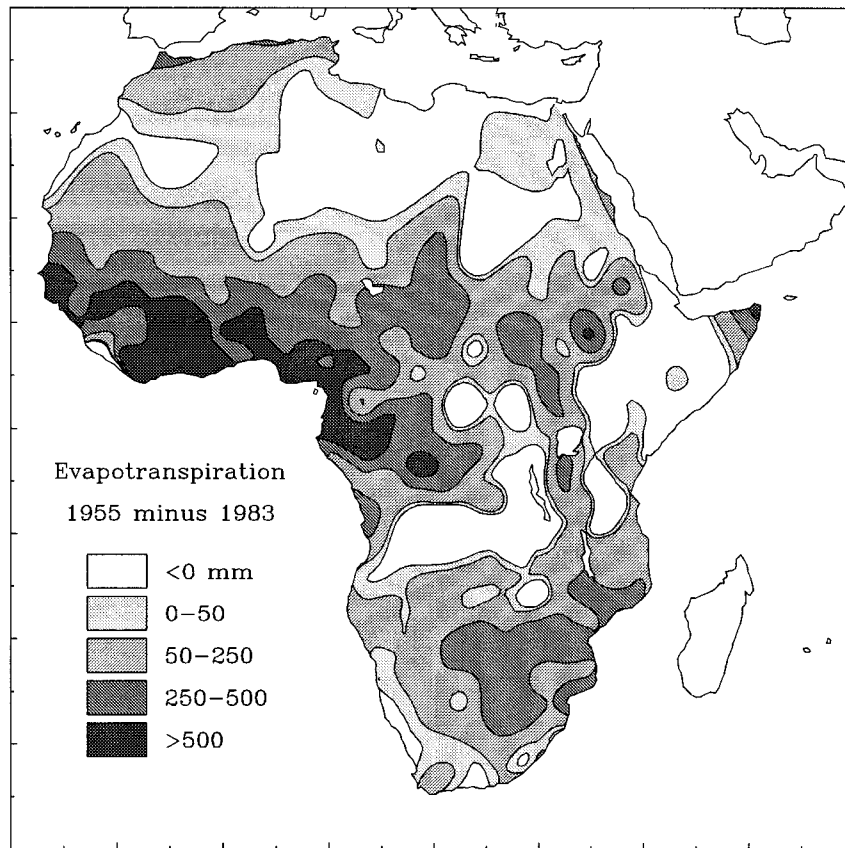
FIG. 10. Difference (in mm) between annual evapotranspiration in 1955 and 1983,
continentally an exceedingly wet and an exceedingly dry year, respectively.

Runoff is calculated using the assumption that rainfall is the only variable that fluctuates from year to year. This is not strictly valid, as solar radiation certainly changes significantly from year to year and smaller changes in surface albedo and NDVI are observed. However, over Africa, solar radiation varies by about 5% to 10% of the mean (BN97), while the fluctuations of rainfall are several times larger. Moreover, the model is considerably more sensitive to precipitation than to solar radiation (Lare and Nicholson 1990) and, because radiation is the limiting factor in few African locations, an increase in solar radiation generally has little effect on water balance (Marengo et al. 1996; Lare and Nicholson 1990). For this reason, it is justifiable to calculate the interannual variability in runoff (Fig. 13) by allowing only precipitation to vary from year to year.

The zone from 10 N to 20 N is the only one where a strong trend in either variable is evident over this 40-yr period. Both rainfall and runoff show a steady downward trend over this period, with a marked decrease occurring around 1970. This zone encompasses the Sahel–Soudan region of West Africa, where the long downward trend is well known (e.g., Nicholson and Palao 1993). There is some semblance of this trend in the two equatorial zones (0 to 10 N and 0 to 10 S), but an increase is apparent in rainfall and runoff in both zones in the mid- to late 1980s. In the outer Tropics of the Southern Hemisphere (10 to 20 S), there is a general downward trend over the 40-yr period, as in the same latitudes of the Northern Hemisphere, but here rainfall and runoff begin to decrease earlier (in the mid-1960s), the trend is less steady, and relatively wet conditions interrupt the trend in the mid- and late 1970s. A similar course of rainfall and runoff is apparent farther south in the zone from 20 to 30 S.

Thus, throughout the area from 30 S to 30 N, there is a general trend toward drier conditions during the last few decades, a pattern also described in Nicholson (1994) using individual station data. However, in the extratropical latitudes a generally opposite trend is apparent. The period 1970–89 is somewhat wetter than the two previous decades, with the change in rainfall being more apparent than the change in runoff.

4. Comparison with results of other studies

The most comprehensive global water balance studies are those of Baumgartner and Reichel (1975), Henning (1989), Willmott et al. (1985), and Mintz and Walker

(1993). For several reasons, these are not strictly comparable to our study. For one, only Willmott et al. (1985) present the station distribution. None of these studies indicates the years utilized to calculate water balance or the mean rainfall in these years at the stations in their dataset. [Baumgartner and Reichel (1975) do provide a map of rainfall.] Also, Mintz and Walker (1993) use very coarse grid averages. Nevertheless, a comparison with their results provides some interesting similarities and contrasts.

A more thorough comparison is possible with the Willmott et al. (1985) study by way of a gridded water balance dataset that they produced and archived at the National Center for Atmospheric Research. Like ours, it has a 1   1 resolution and includes rainfall. Unlike the published map, it allows for a comparison of individual months.

For the six individual locations in Figs. 11 and 12, calculations are also carried out with the Thornthwaite and the Penman–Monteith models and compared with our calculations.

a. Evapotranspiration maps

The evapotranspiration maps of Willmott et al. (1985) (henceforth referred to as WRM) and Baumgartner and Reichel (1975) (henceforth referred to as BR), both calculated from Thornthwaite's dataset, show excellent agreement with each other and good agreement with ours. Maximum values are found in the equatorial region and are in the range of 75 to 125 mm month[1] on the WRM map (900 to 1400 mm yr [1]), compared to 1000 to 1500 mm yr [1] on ours. Their core region, with ET in excess of 100 mm month [1], lies close to our 1250 mm yr [1] contour. Differences are more apparent in the higher latitudes. In the central Sahel, at about 15 N, our calculations give approximately 500 mm yr [1], compared to 50 mm month [1] on the WRM map. Near the southern limit of the Sahara at approximately 18 N lies our 200 mm yr [1] contour and their 25 mm month [1] contour. These same contours border the Namib Desert in southern Africa.

Differences of this magnitude can readily be accounted for by the coarse resolution of the WRM map (4 lat   5 long) and the steep gradients in the semiarid transition zones. A comparison with the 1   1 dataset shows differences of a lower magnitude, with our values generally being slightly higher than those of WRM (Fig. 14). In January, there are few areas where the differences exceed 30 mm, but in July, the differences reach 30 to 40 mm throughout the semiarid Sahel–Soudan zones of West Africa. In that case, the calculations of WRM give higher evapotranspiration. In the annual average, the differences are less than 20 mm nearly everywhere. An examination of the precipitation fields used as input to the models shows that most of these differences can be attributed to differences in precipitation, rather than to the method of calculation. This is
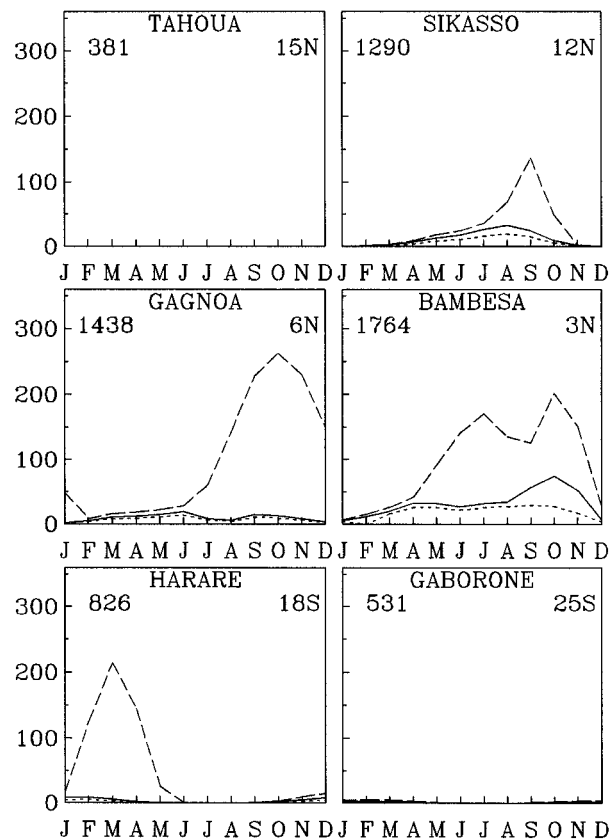

FIG. 11. Monthly runoff (in mm) at six locations in wet years and in dry years. The dashed line indicates the mean for the 10 wettest years during the 1930–90 period, the dotted line indicates the mean for the 10 driest years during this period, and the solid line indicates the mean for the entire period.

particularly true for the Sahel–Soudan zones. The two exceptions are the area about 10 S, where differences exceed 40 mm in January, and the western Guinea Coast, where July differences exceed 30 mm. These differences are roughly 20% to 25% of the monthly evapotranspiration and cannot be accounted for by precipitation input into the respective models.

Our evapotranspiration calculations also show excellent agreement with those of Mintz and Walker (1993) (henceforth referred to as MW). Their annual map indicates that ET reaches about 1100 mm yr [1] in the equatorial regions, in reasonably good agreeement with our values of about 1250 mm. On the July map, the 3 mm day [1] contour bounding the area of maximum ET coincides with our 100 mm month [1] contour, encompassing the area between about 3 and 16 N; MW show the 2 mm day [1] contour at about 18 N, roughly the location of our 50 mm month [1] contour. Both are located at about 5 S in the Southern Hemisphere. In January, the area of maximum moves southward to encompass the area between 2 N and 10 S on the MW map, but extends to about 15 S on our map. Similar agreement is apparent
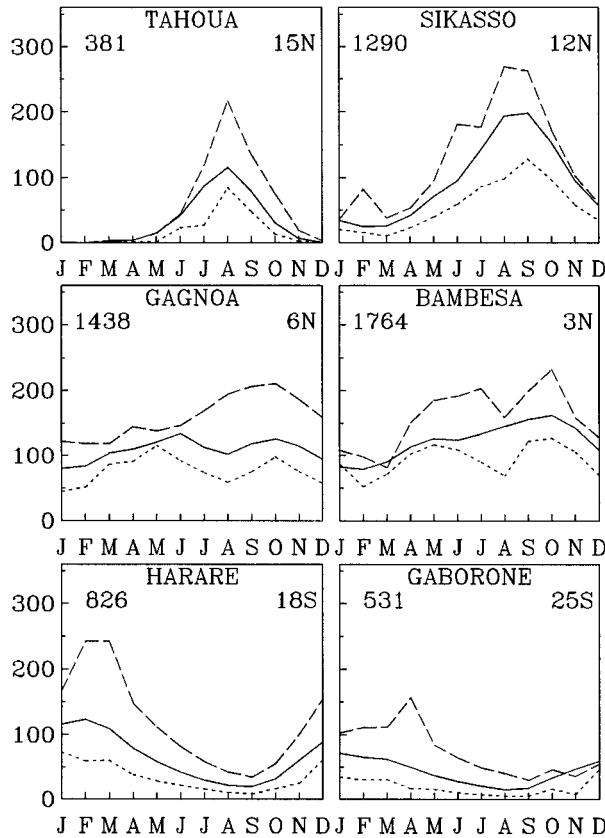
FIG. 12. Monthly evapotranspiration (in mm) at six locations in wet years and in dry years. The dashed line indicates the mean for the 10 wettest years during the 1930–90 period, the dotted line indicates the mean for the 10 driest years during this period, and the solid line indicates the mean for the entire period.
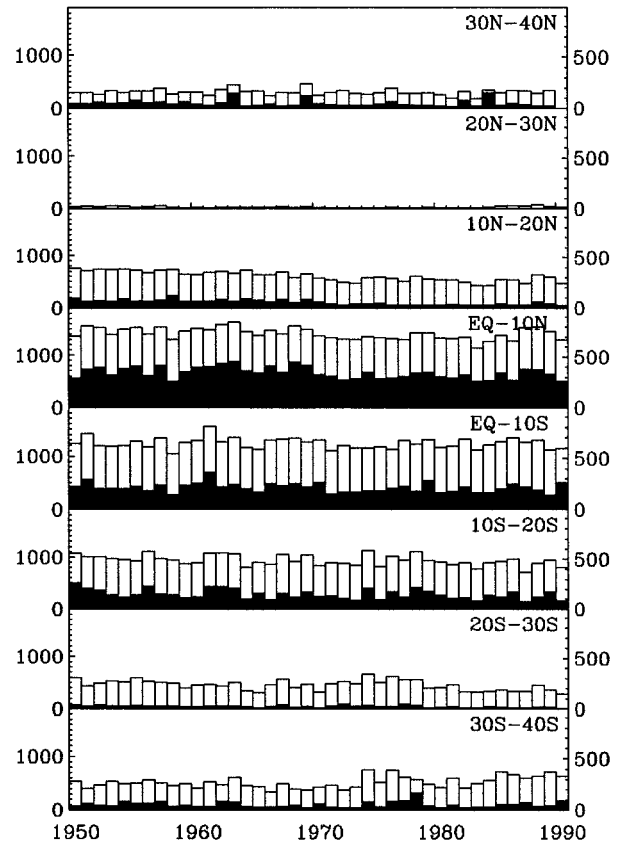

FIG. 13. Zonal averages of rainfall and runoff (mm yr $^{-1}$) over the African continent during the period 1950 to 1989 for each 10° of latitude from 40°N to 40°S. Vertical axis on the right refers to runoff, indicated in solid bars; vertical axis on the left refers to rainfall, indicated in open bars.

in areas of minimum ET as well, particularly in the Southern Hemisphere.

All four estimates are considerably higher than those of Henning (1989), especially in the equatorial belt. Near the southern limit of the equatorial maximum at 5°S, the estimates of WRM and BR and our own indicate about 1400 to 1500 mm yr $^{-1}$, compared to about 1100 mm yr $^{-1}$ on the Henning map. Near 10°N, where the semiarid zone begins, Henning indicates 700–800 mm yr $^{-1}$, compared to 900–1100 mm for the other estimates. One factor contributing to Henning's low estimates are the low values of net radiation he calculates for Africa from empirical formulas; they are considerably lower than satellite estimates (e.g., BN97). The discrepancies are particularly large in arid and semiarid regions, where his surface albedo values are smaller than generally accepted (e.g., 27% throughout the Sahara).

b. Runoff maps

Runoff can be compared with both BR and Henning. On our map, runoff ranges from about 200 to 500 mm yr $^{-1}$ in equatorial latitudes bounded by roughly 8°N and 10°S. A second area with runoff exceeding 200 mm is found along the western Guinea coast, in the area of Sierra Leone and Guinea. This is quite similar to the BR map; however, they show a small core with values exceeding 600 mm yr $^{-1}$, compared with 500 mm yr $^{-1}$ on our map. The location of the desert areas where runoff becomes negligible is also similar on both maps, but our map gives substantially higher runoff in some semiarid regions. In the southern Sahel (approximately 12° to 15°N), our map gives 10 to 50 mm yr $^{-1}$, compared to less then 10 mm yr $^{-1}$ on the map of BR. The Henning calculations exceed these by nearly an order of magnitude in the outer Tropics, but agree reasonably well with BR and with our estimates in the southern equatorial latitudes (approximately 15°S to the equator). However, they give values 5 to 10 times larger in the northern equatorial latitudes to approximately 12°N. Both BR and Henning show a very strong western equatorial maximum over Cameroon, a realistic feature captured in the manual map analysis, but missed in our computer contoured map.

Runoff calculations are extremely difficult to verify. Some confidence in our results can be gained through a
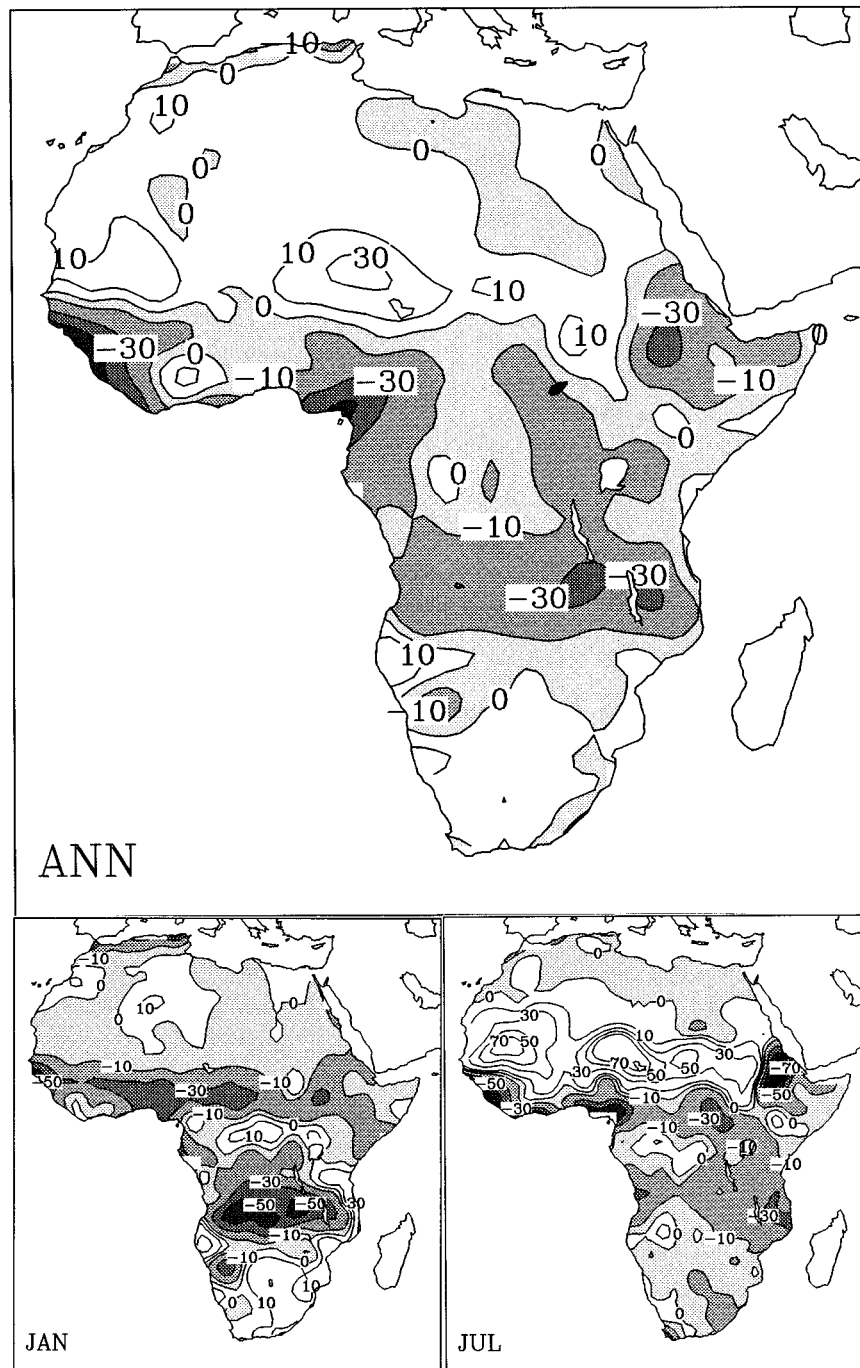
FIG. 14. The difference between the evapotranspiration calculations of WRM and this article. Values are in millimeters, with negative values (shaded) indicating lower ET in the WRM analysis.

rough comparison with river discharge in three diverse parts of Africa. The rivers with available data are the Niger in West Africa, the Zaire in western equatorial Africa, and the tributaries to Lake Victoria in eastern equatorial Africa. Data for these three are plotted in Fig. 15.

In each case, the catchment area was roughly approximated, as indicated in Fig. 15, and average rainfall and runoff for that area were calculated for each year for which discharge data were also available. Then the data were averaged for two subperiods within the record, one constituting relatively dry conditions and the other relatively wet conditions. The resultant differences in rainfall, runoff, and discharge are given in Table 2.

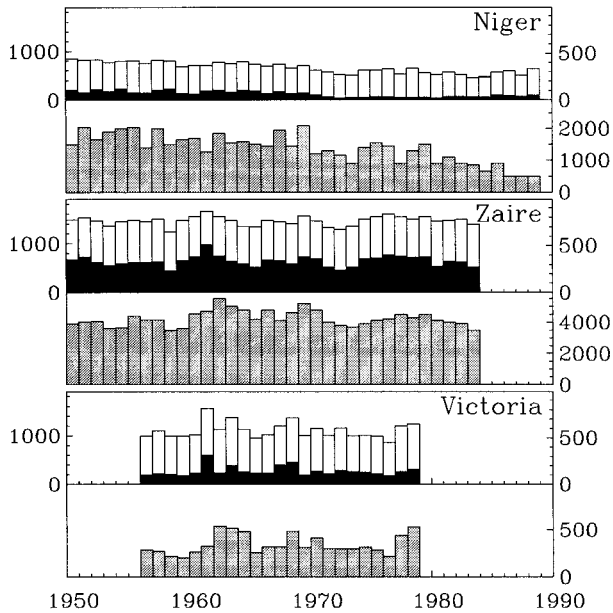Overall, the trends of both rainfall and runoff are

FIG. 15. Time series of annual rainfall, runoff, and river discharge for three basins over Africa (discharge data from Howell et al. 1988; Dümenil et al. 1993). For each basin, the top diagram indicates rainfall (open bars) and runoff (shaded bars) in millimeters, with the left-hand axis referring to rainfall, the right-hand axis referring to runoff, and the bottom diagram indicates discharge (lightly shaded bars). For the Niger and Zaire Rivers, discharge is in m^3 s^{-1}; for the Victoria tributaries, discharge is in millimeters and represents an annual average normalized by the area of the lake. The Niger River discharge is compared with rainfall and runoff in the area bounded by 10 and 20 N and 15 and 0 W. The Zaire River discharge is compared with rainfall and runoff in the area bounded by 5 N and 15 S and by the Atlantic coast and 30 E. The discharge of the Lake Victoria tributaries is compared with rainfall and runoff in the area bounded by 3 N and 5 S and by 30 and 38 E.

markedly similar qualitiatively to that of discharge (Fig. 15). However, the reduction in discharge in the drier period is quantitively closer to that in runoff than that in rainfall. For the Niger River area, rainfall was 62% lower during 1970–88 than during 1950–69, while runoff was 26% lower. River discharge was reduced by 40% during the second period. For the Zaire River, rainfall, runoff, and discharge were not signficantly different in the earlier and later periods, so that shorter wet and dry periods were chosen for comparison. Rainfall and runoff were 2% and 10% lower, respectively, during

TABLE 2. Differences in river discharge, rainfall, and runoff between a relatively wet and a relatively dry period (see Fig. 15). Rainfall and runoff are for areas roughly approximating the catchment areas, as indicated in the caption of Fig. 15. The periods are given in the second column, with negative values for rainfall, runoff, and discharge indicating higher values in the first period.

Basin	Years	Rainfall	Runoff	Discharge
Niger	(1950–69)–(1970–88)	62%	26%	40%
Zaire	(1950–59)–(1960–69)	2%	10%	18%
Victoria	(1956–69)–(1970–78)	13%	5%	0%

TABLE 3. Water balance parameters for 5 latitudinal zones over Africa. First three columns are the annual runoff ratio, the annual evaporation ratio, and annual evapotranspiration, as calculated by this study. The four column is Henning's estimates of evapotranspiration, and the fifth column is Baumgartner and Reichel's estimate of the evaporation ratio.

	N/P	E/P	E (mm)	E_H (mm)	E/P_{BR}
35 –40 N	10	90	594	355	89
30 –35 N	1	99	215	186	105
25 –30 N	0.0	100	23	55	117
20 –25 N	0.0	100	35	58	97
15 –20 N	0.2	100	244	198	97
10 –15 N	5	95	727	517	93
5–10 N	14	86	1193	773	81
Equator–5 N	13	87	1144	846	74
5 S–equator	12	88	1178	958	77
10 –5 S	9	91	1058	880	84
15 –10 S	12	88	1023	772	86
20 –15 S	5	95	730	715	85
25 –20 S	2	98	446	559	91
30 –25 S	3	97	450	428	93
35 –30 S	3	97	441	423	92

1950–59 than during 1960–69, while discharge was 18% lower. For the Lake Victoria area, with a shorter discharge record, rainfall was 13% lower during 1956–69 than during 1970–78, while runoff was 5% lower. The discharge of tributaries into the lake was virtually the same during the two periods. Thus, our runoff estimates are reasonably consistent with discharge data. Better agreement might result if calculations were done for precise catchment areas.

c. Zonal averages

A more precise comparison with BR and Henning can be made using continental and zonal averages, which they present. Table 3 gives, for each 5 of latitude, the average evapotranspiration and the evaporation and runoff ratios as calculated in this study (i.e., the ratios of these quantities to precipitation). For comparison, the zonal averages of ET from Henning and the evaporation ratio from BR are used.

There is reasonably close agreement with BR, except in the equatorial latitudes and at 15 to 20 S, where our evaporation ratios exceed theirs by 10% or more. The difference can be accounted for by the higher rainfall totals on our maps in this region. There is also a discrepancy in the region of the Sahara, but this is considered insignificant in view of the low mean annual rainfall there, on the order of a few tens of millimeters or less in most areas. The discrepancy results in part by BR's addition of evaporation from surface waters in the Saharan region, producing the evaporation ratios that exceed 1.

In contrast, our ET figures greatly exceed those of Henning, by hundreds of millimeters in several cases, but there is reasonably good agreement in the outer Tropics and the subtropics. The low ET of Henning is consistent with the excessively high runoff in their

study. Our ET calculations show a weak relative minimum in equatorial latitudes, a consequence of higher cloudiness in equatorial regions. That feature is not apparent in the ET calculations of Henning.

d. Soil moisture

WRM provide continental estimates of annual mean soil moisture. The soil moisture fields strongly resemble the ET fields in both shape and magnitude. Despite the close agreement between our ET calculations and theirs, there are large differences in soil moisture estimates. In the central Sahel near 15 N, their map indicates mean soil moisture below 25 mm, compared to 50 mm on our map. There is better agreement in the Southern Hemisphere, with 25 mm near 20 S and 50 mm near 15 S on both maps. The biggest discrepancy is in the equatorial latitudes. WRM indicate a core with soil moisture exceeding 75 mm; it exceeds 100 mm in only about half of this area. Our calculations generally give over 200 mm throughout this area, compared with a maximum of about 125 mm in a very small core on the WRM map. The soil moisture values of WRM are fairly low for the equatorial Tropics with year-round rainfall.

Using their 1 1 estimates, we produced maps (not shown) of the differences in mean soil moisture between the two analyses for January, July, and the annual average. The two datasets differ by over 100 mm throughout much of the continent, including nearly the entire equatorial sector. However, the direct model comparison in section 4e indicates that much of the difference can be accounted for by differences in assumed water-holding capacities of soils. WRM use 150 mm for the entire continent, while our estimates vary considerably and generally range between 200 and 500 mm in the equatorial region.

For this reason, a comparison of the two analyses is made by examining the soil ''wetness,'' the ratio of soil moisture to water-holding capacity (Fig. 16). There is excellent agreement on the wet equatorial core where wetness exceeds 75%, but the wetness gradient toward the arid regions is much sharper in the WRM analysis. For example, at about 15 N, it falls to 10% in July on the WRM map, compared to 25% on our map. Similarly, in January, it falls from 75% to 10% within a 5 latitude band on the WRM map, while this drop is spread over 10 of latitude on our map. In the absence of widespread soil moisture measurements, it is difficult to judge which analysis is more accurate. However, our values have been verified for the central Sahel at 13 to 14 N (Marengo et al. 1996). Vegetation information (see section 4e) also suggests that our values are more realistic in these semiarid regions.

The soil wetness maps of MW suggest a higher degree of soil saturation than WRM in the extratropical latitudes and are thus consistent with our results. The similarity with our maps is striking in semiarid areas such as the Sahel of northern Africa and the Kalahari of southern Africa, where soil moisture wetness ranges from 10% to 50% during the wettest months. Both analyses show an annual average in the equatorial region of over 70%. On the MW maps, it reaches 90% in both July and October, but about 70% in January and April. The latitudes of maximum saturation (exceeding 90%) shift from a narrow zone just north of the equator in July to a wide latitudinal band south of the equator in January. The MW and WRM analyses show excellent agreement on the location and size of this zone. Our maps indicate a similar area in January, but a somewhat smaller area in July.

e. Direct comparison with Thornthwaite and Penman–Monteith models

We have carried out a direct comparison between calculations from our model and two other well-known models (Thornthwaite and Penman–Monteith), using the six stations in Figs. 11 and 12. These include two forest locations (Gagnoa and Bambesa), two woodland areas (Sikasso and Harare), and two savanna locations (Tahoua and Gaborone). They also include a contrast between the highly concentrated rainy seasons of the Northern Hemisphere and the longer, less intense rainy seasons of the Southern Hemisphere. The Thornthwaite model is utilized to calculate both ET and soil moisture, but the Penman–Monteith model calculates only ET, using our soil moisture estimates as input.

To facilitate the comparison among the models and to perform a limited senstiivty test, calculations were done utilizing in one model run a water-holding capacity of 150 mm and in a second run 250 mm. Other input values are as described in section 2a. Additional parameters are required for the Penman–Monteith model. These include vegetation parameters (vegetation height, transpirational leaf area, and leaf conductances), with values chosen that are appropriate for the vegetation type at the station (Dingman 1994) and station meteorological parameters (surface pressure, temperature, relative humidity, and wind speed).

The results are shown in Figs. 17a and 17b. For the three driest stations (Tahoua, Harare, and Gaborone), there is excellent agreement between the calculation of ET by our model and that of Thornthwaite (Fig. 17a). The Penman–Monteith model predicts markedly lower ET in the these stations, presumably because it predicts the contribution of the vegetation cover to the total ET and cover is only partial at these stations. For the three wettest stations (Sikasso, Gagnoa, and Bambesa), the Thornthwaite model tends to predict lower values than our model during the wettest months and to reduce the intensity of the seasonal cycle in ET. For these stations, with nearly full vegetation cover, there is somewhat better agreement between the Thornthwaite and Penman–Monteith models. A change in water-holding capacity of the soil appears to have little influence on ET at any of the stations.
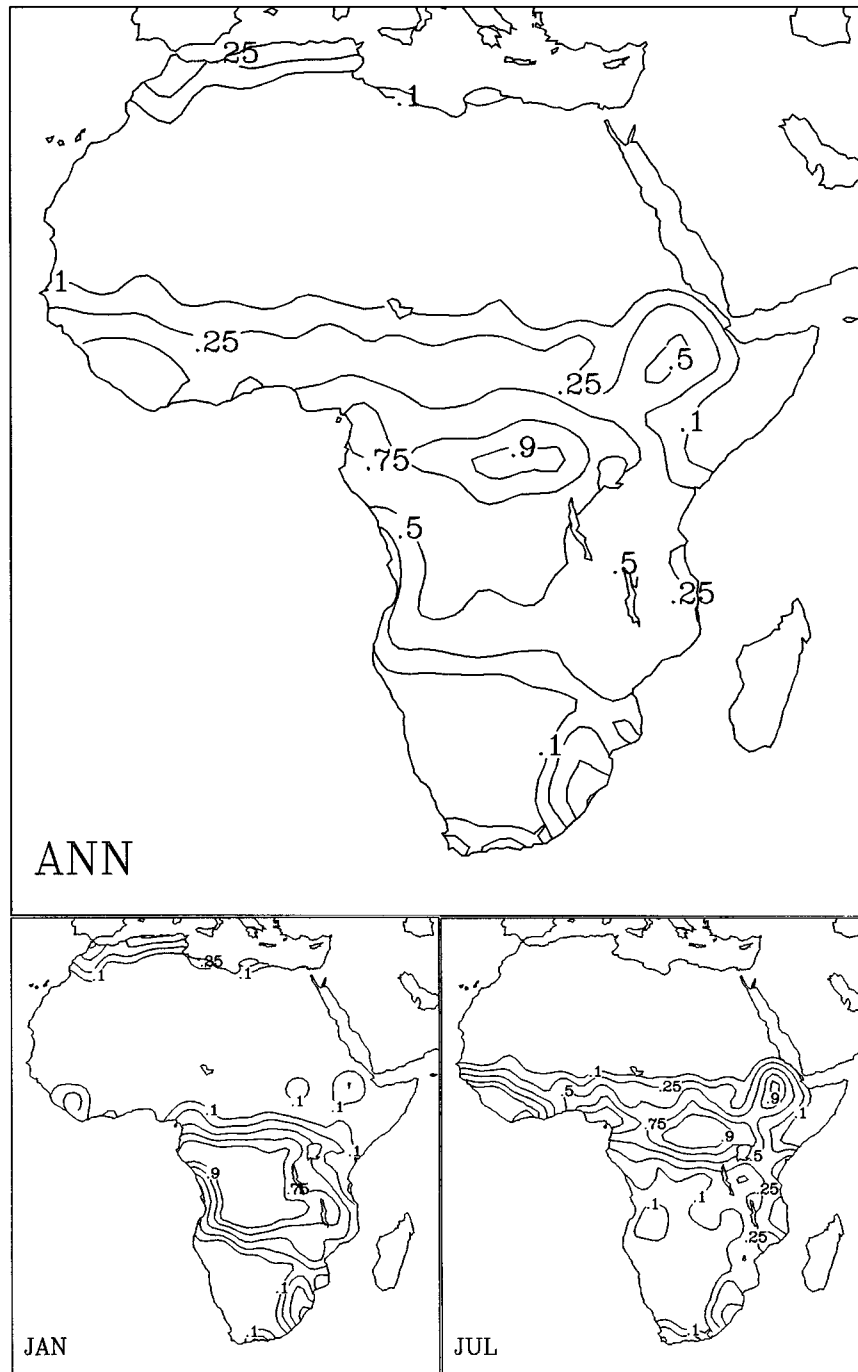
FIG. 16. Maps of soil wetness (the ratio of soil moisture to water-holding capacity) (a) as calculated by WRM and (b) as calculated by our model.

Except for the driest two stations, there is excellent agreement between our model and the Thornthwaite model in soil moisture calculations when water-holding capacity is 150 mm. These results suggest that the discrepancies between our soil moisture calculations and those of WRM are due to differences in assumed water-holding capacity. When water-holding capacity is increased to 250 mm, soil moisture increases markedly in all cases, and the differences between the two models are greater, but the models are still in substantial agreement.

At the driest stations (Tahoua and Gaborone), the Thornthwaite model predicts totally dry soil, compared to peak values of 50 to 100 mm predicted by our model. The nature of the vegetation cover and its density, as
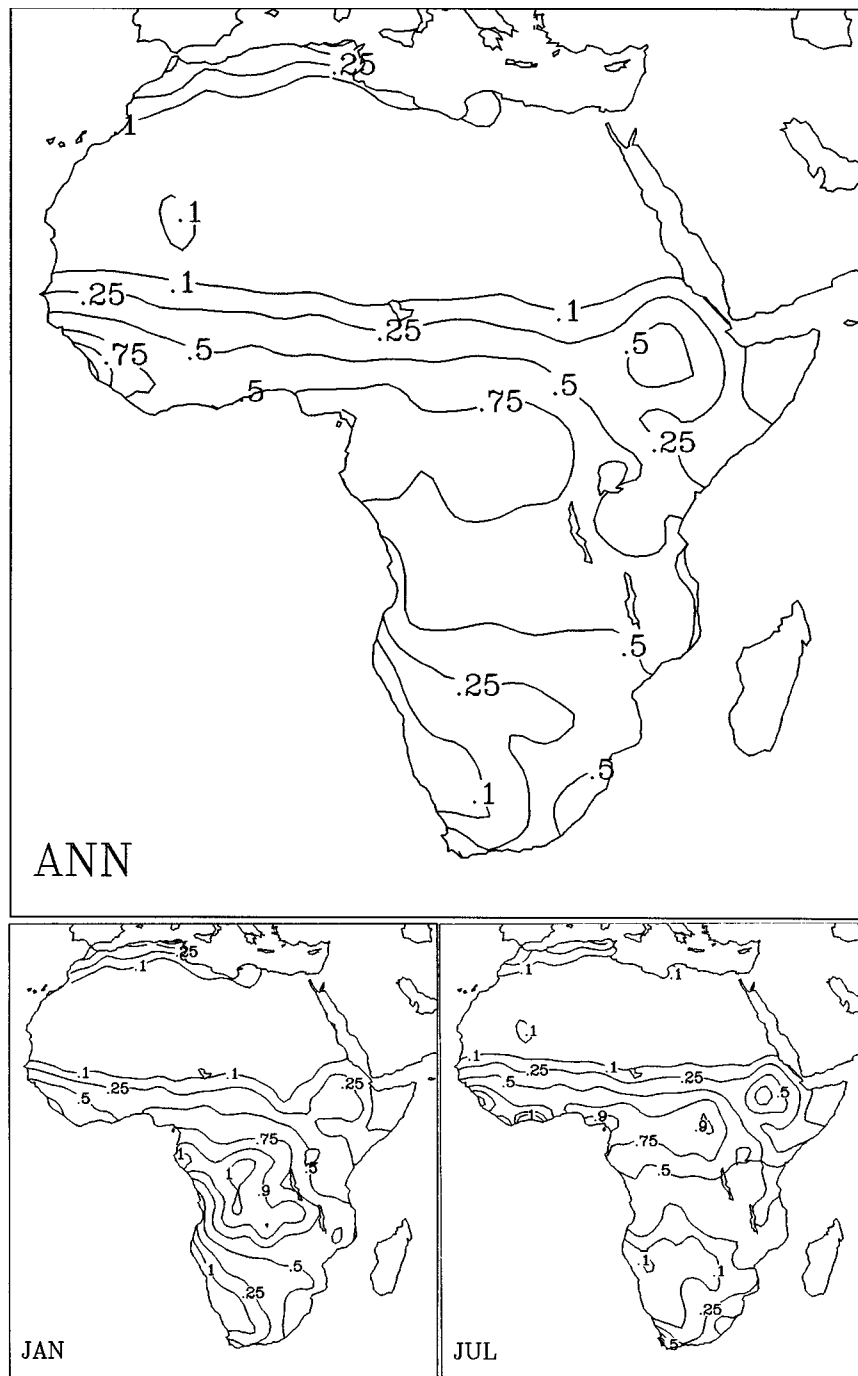
FIG. 16. (*Continued*)

indicated by NDVI, demonstrate that dry soil at these locations is unrealistic (Malo and Nicholson 1990; Grist et al. 1997). Also, soil moisture calculations by our model have been shown to be in marked agreement with the intraseasonal and interannual variability of the vegetation (Farrar et al. 1994; Nicholson et al. 1996a). For Tahoua and Gaborone (Fig. 18), the excellent agreement

between the seasonal cycles of NDVI and calculated soil moisture suggests the validity of our results.

At wetter stations, where water is not the limiting factor and transpiration provides nearly all of the evapotranspiration, NDVI would be expected to show a better relationship to ET than to soil moisture (Nicholson et al. 1996a). Figure 18 compares NDVI at Bambesa and
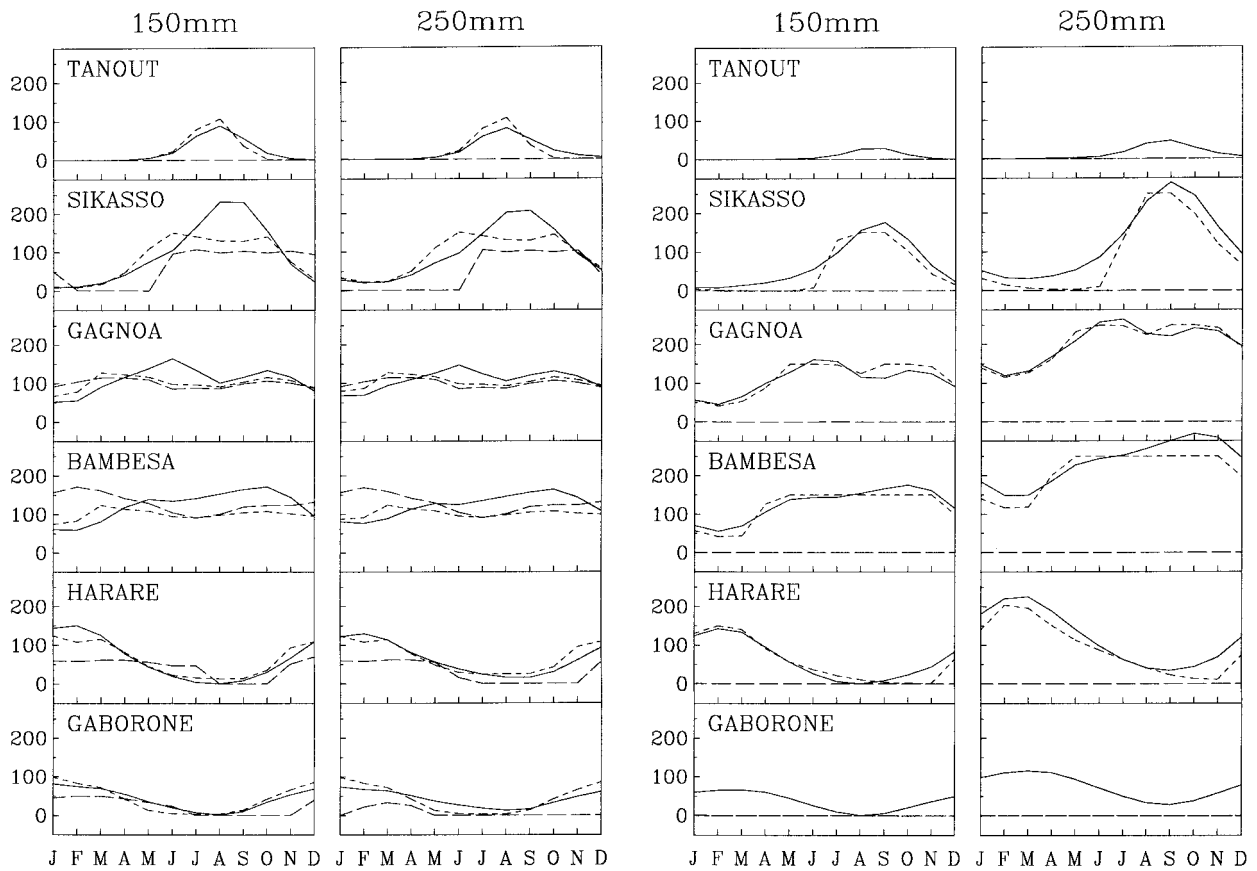
FIG. 17. (a) Model intercomparison: evapotranspiration (mm month [1]) at select stations, as calculated by the climatonomy (solid line), Thornthwaite (dotted line), and Penman–Monteith (dashed line) models. Results on the left are based on a water-holding capacity of 150 mm, and those on the right are based on 250 mm. (b) Model intercomparison: soil moisture (mm) at select stations, as calculated by the climatonomy (solid line), Thornthwaite (dotted line), and Penman–Monteith (dashed line) models. Results on the left are based on a water-holding capacity of 150 mm, and those on the right are based on 250 mm.

Gagnoa to ET, as calculated by our model and that of Thornthwaite. The somewhat better correspondence with our model results suggests that our model might be more realistic in these regions.

5. Summary and conclusions

This study has produced high-resolution estimates of evapotranspiration, runoff, and soil moisture over the African continent. Evapotranspiration generally exceeds 1500 mm yr [1] in the equatorial regions, with a few areas where ET is in excess of 2000 mm yr [1]. It ranges from about 500 to 750 mm yr [1] in the semiarid regions of eastern Africa and from about 200 to 750 mm month [1] in the semiarid regions of the subtropics. On a monthly scale, maxima are on the order of 100 mm month [1] or more. It is on the order of 5 to 50 mm yr [1] in the semiarid regions bordering the deserts. Runoff is about

FIG. 17. (*Continued*)

200 to 500 mm yr [1] in the equatorial latitudes, but is generally less than 50 mm yr [1] in semi arid regions of Africa. It approaches zero for mean annual rainfall below 500 mm.

Interannual variability is particularly large for ET. In some areas, the difference between wet and dry years exceeds 500 mm yr [1]. It can exceed 250 mm yr [1] over much of the continent. Runoff can vary by over 100
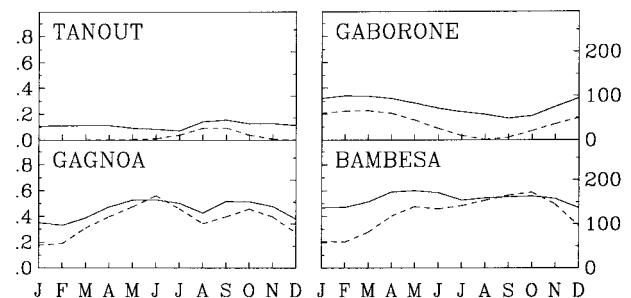

FIG. 18. Comparison between NDVI (solid line, left vertical axis) and climatonomy results (dotted lines, right vertical axis). Left: comparison with soil moisture (mm) calculated for Tahoua and Gaborone. Bottom, comparison with evapotranspiration (mm month [1]) calculated for Gagnoa and Bambesa. The NDVI values include a baseline of background effects, such that bare ground corresponds to a value of roughly 0.1.

mm yr^{1} from year to year in wetter regions of West Africa. In the equatorial latitudes, even zonal means can vary by over 200 mm yr^{1}, compared to a long-term mean on the order of 350 mm yr^{1}. In the semiarid subequatorial latitudes, the zonal means can vary by 100 to 150 mm yr^{1}.

Overall, there is good agreement between our calculations of ET and those of several other studies. Nevertheless, a considerable range of values for the African continent appears in the literature. Some earlier studies appear to have dramatically underestimated ET. This is partly a consequence of the relatively low values of net radiation obtained from traditional formulas, as compared to modern satellite estimates. Differences in assumed surface albedo, particularly in desert areas such as the Sahara, are a contributing factor.

There is less agreement in the case of soil moisture, although our values are consistent with the recent estimates of Mintz and Walker (1993). The discrepancies between our calculations and those of Willmott et al. (1985), based on the Thornthwaite model, appear to be due primarily to differences in assumed water-holding capacity of the soils. Except in semiarid regions, the agreement at sample stations is excellent if both models utilize the same water-holding capacity. However, our model produces higher and more realistic soil moisture values in the semiarid regions. These results dramatically underscore the need for accurate soils information for the assessment of water balance on a continental scale.

REFERENCES

Albrecht, F., 1951: Die Methoden zur Bestimmung der Verdunstung der natürichen Erdoberfläche. *Arch. Meteor. Geophys. Bioklimatol., Ser. B,* **III,** 1–38.

——, 1962: Die Berechnung der natürlichen Verdunstung (evapotranspiration) der Erdoberfläche aus klimatologischen Daten. *Ber. Dtsch. Wetterdienstes,* Vol. 14, 54 pp.

Ba, M. B., R. Frouin, and S. E. Nicholson, 1995: Satellite-derived interannual variability of West African rainfall 1983–88. *J. Appl. Meteor.,* **34,** 411–431.

Baumgartner, A., and E. Reichel, 1975: *The World Water Balance.* R. Oldenbourg, 179 pp.

Brubaker, K., D. Entekhabi, and P. Eagleson, 1993: Estimation of continental precipitation recycling. *J. Climate,* **6,** 1077–1089.

Chahine, M. T., 1992a: GEWEX: The Global Energy and Water Cycle Experiment. *Eos, Trans. Amer. Geophys. Union,* **73,** 9–14.

——, 1992b: The hydrologic cycle and its influence on climate. *Nature,* **359,** 9–14.

Dingman, S. L., 1994: *Physical Hydrology.* Macmillan, 575 pp.

Dorman, J. L., and P. J. Sellers, 1989: A global climatology of albedo, roughness length, and stomatal resistance for atmospheric general circulation models as represented by the Simple Biosphere Model (SiB). *J. Appl. Meteor.* **28,** 833–855.

Dümenil, L., K. Isele, H.-J. Liebscher, U. Schröder, M. Schumacher,

and K. Wilke, 1993: Discharge data from 50 selected rivers for GCM validation. Max-Planck-Institut für Meteorologie and Global Runoff Data Center Rep. 100, 61 pp.

Entekhabi, D., I. Rodriguez-Iturbe, and R. Bras, 1992: Variability in large-scale water balance with a land surface–atmosphere interaction. *J. Climate,* **5,** 798–813.

FAO, 1984: *Agroclimatological Data.* Africa Food and Agricultural Organization.

Farrar, T. J., S. E. Nicholson, and A. R. Lare, 1994: The influence of soil type on the relationships between NDVI, rainfall and soil moisture in semi-arid Botswana. Part II. NDVI response to soil moisture. *Remote Sens. Environ.,* **50,** 121–133.

Grist, J., S. E. Nicholson, and A. Mpolokang, 1997: On the use of NDVI for estimating rainfall fields in the Kalahari of Botswana. *J. Arid Environ.,* **35,** 195–214.

Henning, D., 1989: *Atlas of the Surface Heat Balance of the Continents.* Gebrüder Borntraeger, 402 pp.

Howell, P., M. Lock, and S. Cobb, 1988: *The Jonglei Canal: Impact and Opportunity.* Cambridge University Press, 537 pp.

Lare, A. R., 1992: An investigation into land-surface feedback and the African drought using climatonomy modeling. Ph.D. dissertation, The Florida State University, 333 pp. [Available from Dept. of Meteorology, The Florida State University, Tallahassee, FL 32306.]

——, and S. E. Nicholson, 1990: A climatonomic description of the surface energy balance in the central Sahel. Part I: Shortwave radiation. *J. Appl. Meteor.,* **29,** 123–137.

——, and ——, 1994: Contrasting conditions of surface water balance in wet and dry years as a possible land surface–atmosphere feedback mechanism in the West African Sahel. *J. Climate,* **7,** 653–668.

Lettau, H. H., 1969: Evapotranspiration climatonomy. I. A new approach to numerical prediction of monthly evapotranspiration, runoff and soil moisture storage. *Mon. Wea. Rev.,* **97,** 691–699.

——, and M. W. Baradas, 1973: Evapotranspiration climatonomy II: Refinement of parameterizations exemplified by application to the Mabacan River watershed. *Mon. Wea. Rev.,* **101,** 636–649.

Malo, A. R., and S. E. Nicholson, 1990: A study of rainfall and vegetation dynamics in the African Sahel using normalized difference vegetation index. *J. Arid Environ.,* **19,** 1–24.

Marengo, J. A., S. E. Nicholson, A. R. Lare, B. Monteny, and S. Galle, 1996: Application of evapoclimatonomy to monthly surface water balance calculations at the HAPEX-Sahel supersites. *J. Appl. Meteor.,* **35,** 562–573.

Mather, J. R., 1962: Average climatic water balance data on the continents: part 1. Africa. *Publ. Climatol.,* **15**(2).

——, 1963a: Average climatic water balance data on the continents: part 2. Asia (excluding U.S.S.R.). *Publ. Climatol.,* **16**(1).

——, 1963b: Average climatic water balance data on the continents: part 3. U.S.S.R. *Publ. Climatol.,* **16**(2).

——, 1963c: Average climatic water balance data on the continents: part 4. Australia. *Publ. Climatol.,* **16**(3).

——, 1964a: Average climatic water balance data on the continents: part 5. Europe. *Publ. Climatol.,* **17**(1).

——, 1964b: Average climatic water balance data on the continents: part 6. North America (excluding United States). *Publ. Climatol.,* **17**(2).

——, 1964c: Average climatic water balance data on the continents: part 7. United States. *Publ. Climatol.,* **17**(3).

——, 1965: Average climatic water balance data on the continents: part 8. South America. *Publ. Climatol.,* **18**(2).

Mintz, Y., and G. K. Walker, 1993: Global fields of soil moisture and land surface evapotranspiration derived from observed precipitation and surface air temperature. *J. Appl. Meteor.,* **32,** 1305–1334.

Nicholson, S. E., 1989: African drought: Characteristics, casual theories and global teleconnections. *Understanding Climate Change,* A. Berger, R. E. Dickinson, and J. W. Kidson, Eds., Amer. Geophys. Union, 79–100.

——, 1994: Recent rainfall fluctuations in Africa and their relation-

ship to past conditions over the continent. *Holocene,* **4,** 121–131.

——, and A. R. Lare, 1990: A climatonomic description of the surface energy balance in central Sahel. Part II: The evapoclimatonomy submodel. *J. Appl. Meteor.,* **29,** 138–146.

——, and I. Palao, 1993: A re-evaluation of rainfall variability in the Sahel. Part I. Characteristics of rainfall fluctuations. *Int. J. Climatol.,* **13,** 371–389.

——, and T. J. Farrar, 1994: The influence of soil type on the relationships between NDVI, rainfall and soil moisture in semi-arid Botswana. Part I. NDVI response to rainfall. *Remote Sens. Environ.,* **50,** 107–120.

——, A. R. Lare, J. A. Marengo, and P. Santos, 1996a: A revised version of Lettau's evapoclimatonomy model. *J. Appl. Meteor.,* **35,** 549–561.

——, J. Kim, and M. Ba, 1996b: Rainfall in the Sahel during 1994. *J. Climate,* **9,** 1673–1676.

——, J. A. Marengo, J. Kim, A. R. Lare, S. Galle, and Y. H. Kerr, 1997: A daily resolution evapoclimatonomy model applied to surface water balance calculations at the HAPEX-Sahel supersites. *J. Hydrol.,* **188/189,** 946–964.

Pitman, A. J., and Coauthors, 1993: PILPS: Results from off-line control simulations (Phase 1a). WCRP/IGPO Publ. Series 7, 47 pp.

Rawls, W. J., and D. Brakenziek, 1989: Estimation of soil water retention and hydraulic properties. *Unsaturated Flow in Hydrologic Modeling: Theory and Practice,* H. J. Morel-Seytoux, Ed., Kluwer Academic Publishers, 275–300.

Saxton, K. E., W. J. Rawls, J. S. Romberger, and R. J. Papendick, 1986: Estimating generalized soil-water characteristics from texture. *Soil Sci. Soc. Amer., J.,* **50,** 1031–1036.

Serafini, Y. V., and Y. C. Sud, 1987: The time-scale of the soil hydrology using a simple water budget model. *J. Climatol.,* **7,** 585–591.

Walsh, J. E., W. H. Jasperson, and B. Ross, 1985: Influence of snow cover and soil moisture on monthly air temperature. *Mon. Wea. Rev.,* **113,** 756–768.

Warrilow, D., 1986: The sensitivity of the UK Meteorological Office atmospheric general circulation model to recent changes in the parameterization of hydrology. *Proc. ISLSCP Conf.,* Rome, Italy, ESA, 143–149.

Webb, R. S., C. E. Rosenzweig, and E. R. Levine, 1991: A global data set of soil particle size properties. NASA Tech. Memo. 4286, 33 pp.

Webster, P. J., 1994: The role of hydrological processes in ocean–atmosphere interactions. *Rev. Geophys.,* **32,** 427–476.

Willmott, C. J., C. N. Rowe, and Y. Mintz, 1985: Climatology of the terrestrial seasonal water cycle. *J. Climatol.,* **5,** 589–606.

Zobler, L., 1986: A world soil file for global climate modeling. NASA Tech. Memo. 87802, 76 pp.